Eur. Phys. J. B **57**, 37–44 (2007)
DOI: 10.1140/epjb/e2007-00152-1

THE EUROPEAN PHYSICAL JOURNAL B

# Temperature dependence of the cyclotron mass in ZnCdSe/ZnSe multi-QWs

R. Charrour[a] and D. Bria

Laboratoire de Dynamique et d'Optique des Matériaux, Département de Physique, Faculté des Sciences, Université Mohammed I, Oujda Morocco

Received 26 December 2006 / Received in final form 17 April 2007
Published online 25 May 2007 – 

**Abstract.** The temperature dependence of the cyclotron resonance mass (CRM) of the magnetopolaron in ZnCdSe/ZnSe multi-quantum wells with strong magnetic field is investigated theoretically using the Lee-Low-Pines variational method. The contributions to the CRM due to the nonparabolicity of the conduction band and the coupling of electron with both confined longitudinal optical and interface optical phonons are considered. Results of our calculations are compared with the experimental data, and a qualitative agreement is found over a large temperature range. We show that these three contributions complement each other to determine the cyclotron mass as a function of the temperature.

**PACS.** 76.40.+b Diamagnetic and cyclotron resonances – 78.55.Et II-VI semiconductors – 72.10.Fk Scattering by point defects, dislocations, surfaces, and other imperfections

## 1 Introduction

In recent years wide gap II–VI semiconductor heterostructures have attracted much attention mostly in light of their potential for the development of opto-electronic devices operating in the blue-green spectral region [1–4]. II–VI semiconductors are interesting materials also from the viewpoint of the electron-phonon interaction, which gives rise to a relatively large polaron effect.

Special attention is focused on the cyclotron-resonance mass of an electron in II–VI compounds. It is interpreted on basis of the electron-phonon interaction. The cyclotron resonance mass can be obtained from the position of certain peaks in the magneto-optical absorption spectrum [5]. Recent progress in high magnetic field technology has provided the possibility to study cyclotron resonance over a wide range of photon energies and temperatures. Several works on the cyclotron resonance (CR) have been done both experimentally [6–9] and theoretically [10–13] in the 3D and low dimensional systems. The temperature dependence of the cyclotron resonance mass has been investigated theoretically by many authors, but the existing theories are still controversial. Different theoretical methods applied have led to significantly different predictions for the behavior of the cyclotron mass as a function of the temperature.

Taking into account the interaction of an electron with both bulk longitudinal-optical and interface-optical (IO) phonons, Wei and Gu [13] have investigated the cyclotron mass of magnetopolaron in quasi-two-dimensional systems at finite temperature using the generalized Larsen perturbation theory method. The results show that the cyclotron mass is a monotonic function of the temperature. However, with the Green's function method [12], the cyclotron resonance mass of interface magnetopolarons is shown to be an increasing function of temperature when the magnetic field is lower than a resonant magnetic field, but it is a decreasing function of the temperature when the magnetic field is higher than a resonant magnetic field. A different result as compared to the aforementioned temperature dependencies of the cyclotron mass was obtained by extending Feynman's polaron theory [14] to finite temperatures. With this theory it was found that with increasing temperature the cyclotron mass first increases at low temperature, subsequently reaches a maximum value at a certain temperature, and at still higher temperature starts to decrease. For high magnetic fields the theoretical efforts aimed at investigating the cyclotron resonance mass of magnetopolaron have been carried out using the memory-function formalism by Devreese and his associates [10,11]. This method is applied to interpret the experiments of Miura and his co-workers in the bulk $n$-type CdS [6]. A large amount of theoretical work has been done [15–17] concerning the effects of interface phonons on the position of the cyclotron resonance peak. More recently the resonant magnetopolaron effect due to the interaction between the electrons and the interface optical phonon modes were observed experimentally [18].

In this work, using the modified Lee-Low-Pines (LLP) variational method [19], we present a theoretical

[a] e-mail: charrour@telenet.be

calculation of the magnetopolaron cyclotron resonance mass at high magnetic fields with taking into account the interaction of an electron with both confined longitudinal optical (LO) phonons and interface optical (IO) phonons. The calculations are performed for ZnCdSe/ZnSe multi-quantum wells (MQWs) in order to interpret the experimental data of Imanaka and Miura [9]. Our calculations take into account the non-parabolicity of the conduction band. This consideration leads to the following anisotropy of the effective mass: the effective mass in the $xy$-plane is affected by the non-parabolicity 2–3 times more than that along the $z$-direction.

The present paper is organized as follows. In Section 2, a modified Lee-Low-Pines variational technique is presented. Section 3 contains our numerical results. The conclusion is given in the last section.

## 2 Theoretical model

Within the effective-mass approximation, the Hamiltonian of an electron in multi-quantum well system, interacting with both the confined LO phonons and IO phonons, and applied to a uniform magnetic field along the growth direction ($z$-axis), is written as:

$$H = H_e + H_{ph} + H_{e-ph}. \tag{1}$$

Focusing on the nonparabolicity of the conduction band, the electronic Hamiltonian $H_e$ reads in the $\vec{k}\cdot\vec{p}$ theory [20] as:

$$\begin{aligned} H_e = {} & \frac{(\vec{P}+\frac{e}{c}\vec{A})^2}{2m_e^*} + V_w(z) + a_{13}K^4 + a_{14}\big[\{k_x,k_y\}^2 \\ & + \{k_y,k_z\}^2 + \{k_z,k_x\}^2\big] \\ & - a_{15}\left(\frac{e}{\hbar c}\right)B^2 + \left(\frac{\hbar c}{2e}\right)\mu_B g\left(\frac{e}{\hbar c}\right)B\sigma_z \\ & + a_{43}\left(\frac{e}{\hbar c}\right)K^2 B\sigma_z + a_{45}\left(\frac{e}{\hbar c}\right)k_z^2 B\sigma_z \\ & + a_{44}\left(\frac{e}{\hbar c}\right)B[\{k_x,k_z\}^2\sigma_x + \{k_y,k_z\}^2\sigma_y] \\ & + a_{42}[\{(k_y^2-k_z^2)k_x\}\sigma_x \\ & + \{(k_z^2-k_x^2)k_y\}\sigma_y + \{(k_x^2-k_y^2)k_z\}\sigma_z]. \end{aligned} \tag{2}$$

The potential vector $\vec{A}$ is chosen in the symmetric gauge, i.e. $\vec{A} = B(-y,x,0)/2$. $K = (k_x,k_y,k_z)$ is the electron wave vector. $\sigma = (\sigma_x,\sigma_y,\sigma_z)$ are the Pauli spin matrices and $\mu_B$ is the Bohr magneton. The nonparabolicity parameters $a_{ij}$ and their numerical values [21] are determined from a 14-band $\vec{k}\cdot\vec{p}$ calculation. To simulate the effect of multiple wells, we take $V_w(z)$ to be a periodic one-dimensional rectangular-well potential.

$$V_w(z) = \begin{cases} 0; & -\frac{L}{2}+n(L+b) < z < \frac{L}{2}+n(L+b) \\ V_0; & \frac{L}{2}+n(L+n) < z < -\frac{L}{2}+(n+1)(L+b) \end{cases} \tag{3}$$

$L$ is the well width, $b$ is the barrier width, $V_0$ is the barrier height and $n$ is an integer, while the second term in equation (1) is the total Hamiltonian of the free phonon field:

$$H_{ph} = H_{LO} + H_{IO}, \tag{4}$$

where

$$H_{LO} = \sum_{k,m,p} \hbar\omega_{LO} a^+_{m,p}(k)a_{m,p}(k), \tag{5}$$

is the Hamiltonian operator for confined LO-phonons, $a^+_{m,p}(k)[a_{m,p}(k)]$ is the creation (annihilation) operator for a LO phonon with frequency $\omega_{LO}$ and $k$ is the two-dimensional projection on the $xy$-plane of the wave vector. The parity index, $p = \pm$, refers to the miror symmetry with respect to the plane $z = 0$, $m$ is the quantum number related to the $z$-component of the LO-phonon wave vector.

The Hamiltonian operator for IO-phonons is

$$H_{IO} = \sum_{q,\sigma,p} \hbar\omega_{\sigma p} b^+_{\sigma,p}(q)b_{\sigma,p}(q), \tag{6}$$

where $b^+_{\sigma,p}(q)[b_{\sigma,p}(q)]$ is the creation (annihilation) operator for the IO-phonon with frequency $\omega_{\sigma p}$ and the wave vector $q$, where $\sigma = \pm$ refers to the high- and low-frequency IO phonon modes, respectively. $p$ has the same meaning as before. According to Wendler and Pechstedt [22], there are four interface phonon modes with frequencies, $\omega_{++}$, $\omega_{+-}$, $\omega_{-+}$, $\omega_{--}$.

The last term in equation (1) describes the interaction Hamiltonian of an electron with different phonon modes:

$$H_{e-ph} = H_{e-LO} + H_{e-IO}. \tag{7}$$

The first term corresponds to the electron-LO-phonon interaction [23]

$$\begin{aligned} H_{e-LO} = \sum_k \Bigg[ & A^* \exp(-ik\rho)\left[\sum_{m=1,3,..}^{\frac{L}{2a}} \frac{\cos(\frac{m\pi z}{L})}{\left[k^2+\left(\frac{m\pi}{L}\right)^2\right]^{\frac{1}{2}}}\right. \\ & \left.\times a^+_{m,+}(k) + \sum_{m=2,4,..}^{\frac{L}{2a}} \frac{\sin(\frac{m\pi z}{L})}{\left[k^2+\left(\frac{m\pi}{L}\right)^2\right]^{\frac{1}{2}}} a^+_{m,-}(k)\right] + H.c.\Bigg], \end{aligned} \tag{8}$$

where

$$A^* = i\left[\frac{4\pi e^2}{V}\hbar\omega_{LO}\left(\frac{1}{\epsilon_\infty}-\frac{1}{\epsilon_0}\right)\right]^{1/2}, \tag{9}$$

$V$ is the crystal volume and $a$ is the lattice constant. The second term in equation (7) is the electron-IO phonon interaction [24], given by:

$$H_{e-IO} = \sum_{q,\sigma,p}[W_{q,\sigma,p}(z)\exp(iq\rho)b_{\sigma,p}(q) + H.c.], \tag{10}$$

$$\begin{aligned} W_{q,\sigma,+}(z) = -i & \left[2\xi^2_{1\sigma+}\tanh\left(\frac{qL}{2}\right) + 2\xi^2_{2\sigma+}\right]^{-1/2} \\ & \times\left(\frac{2\pi\hbar e^2}{Sq\omega_{\sigma+}}\right)^{1/2}\frac{\cosh(qz)}{\cosh\left(\frac{qL}{2}\right)}, \end{aligned} \tag{11}$$

$$W_{q,\sigma,-}(z) = -i\left[2\xi_{1\sigma-}^2 \coth\left(\frac{qL}{2}\right) + 2\xi_{2\sigma-}^2\right]^{-1/2} \times \left(\frac{2\pi\hbar e^2}{Sq\omega_{\sigma-}}\right)^{1/2} \frac{\sinh(qz)}{\sinh\left(\frac{qL}{2}\right)}, \quad (12)$$

$$\xi_{\lambda\sigma p} = \frac{\varepsilon_{\lambda\sigma p} - \epsilon_{\infty\lambda}}{\omega_{TO\lambda}(\epsilon_{0\lambda} - \epsilon_{\infty\lambda})^{1/2}}; \lambda = 1, 2, \quad (13)$$

$$\varepsilon_{\lambda\sigma p} = \epsilon_{\infty\lambda}\frac{\omega_{LO\lambda}^2 - \omega_{\sigma p}^2}{\omega_{TO\lambda}^2 - \omega_{\sigma p}^2}; \lambda = 1, 2, \quad (14)$$

$\omega_{LO1}(\omega_{LO2})$ and $\omega_{TO1}(\omega_{TO2})$ are the longitudinal and tranverse optical phonon frequencies respectively, for the well (barrier) material.

We apply the variational technique developed by Lee-Low-Pines, to calculate the eigenstates of the Hamiltonain (1). We perform two unitary transformations [23]:

$$U_1 = \exp[-i\sum_{k,m,p} a_{m,p}^+(k)a_{m,p}(k)k\rho - i\sum_{q,\sigma,p} b_{\sigma,p}^+(q)b_{\sigma,p}(q)q\rho] \quad (15)$$

and

$$U_2 = \exp[\sum_{k,m,p}(a_{m,p}^+(k)f_{m,p}(k) - a_{m,p}(k)f_{m,p}^*(k)) + \sum_{q,\sigma,p}(b_{\sigma,p}^+(q)g_{\sigma,p}(q) - b_{\sigma,p}(q)g_{\sigma,p}^*(q))], \quad (16)$$

$f_{m,p}(k), f_{m,p}^*(k), g_{\sigma,p}(q)$ and $g_{\sigma,p}^*(q)$ are the variational parameters, which are determined by minimizing the energy of the system.

At finite temperature, we choose $|N_{m,p}(k), N_{\sigma,p}(q)\rangle$ as the wave function for describing the phonon state, in which $N_{m,p}(k)$ and $N_{\sigma,p}(q)$ represent the number of LO and IO-phonons, respectively. When the temperature is lower than the room temperature, though the phonon frequencies will decrease with increasing temperature, we can still take them as constant because of the small relative change of the frequency [25]. Also, the energies of the interaction between the electron and the phonons are much smaller than the phonon energy except in the strong-coupling case. Accordingly, we may assume that the eigenvalues of $a_{m,p,k}^+ a_{m,p,k}$ and $b_{\sigma,p,q}^+ b_{\sigma,p,q}$ in the phonon state are approximately equal to the equilibrium values [26], i.e.

$$\langle N_{m,p,k}|a_{m,p,k}^+ a_{m,p,k}|N_{m,p,k}\rangle = \eta_{LO} = \frac{1}{\exp\left(\frac{\hbar\omega_{LO}}{k_B T}\right) - 1}, \quad (17)$$

$$\langle N_{\sigma,p,q}|b_{\sigma,p,q}^+ b_{\sigma,p,q}|N_{\sigma,p,q}\rangle = \eta_{\sigma p} = \frac{1}{\exp\left(\frac{\hbar\omega_{\sigma p}}{k_B T}\right) - 1}, \quad (18)$$

where $k_B$ is the Boltzmann constant.

The wave function of the system is chosen far from the resonance as follows:

$$|\psi(z,\rho,k,q)\rangle = |\phi_e(z,\rho)\rangle \prod_{m,p,k}|N_{m,p}(k)\rangle \prod_{\sigma,p,q}|N_{\sigma,p}(q)\rangle, \quad (19)$$

where $\phi_e(z,\rho)$ is the wave function of the electron moving inside of the MQW. The expectation value of the Hamiltonian H with the trial wave function is:

$$E = \langle\psi(z,\rho,k,q)|U_2^{-1}U_1^{-1}HU_1U_2|\psi(z,\rho,k,q)\rangle = \langle\phi_e(z,\rho)|F|\phi_e(z,\rho)\rangle, \quad (20)$$

where

$$F = \prod_{m,p,k}\prod_{\sigma,p,q}\langle N_{m,p}(k), N_{\sigma,p}(q)|U_2^{-1}U_1^{-1} \times HU_1U_2|N_{m,p}(k), N_{\sigma,p}(q)\rangle. \quad (21)$$

After the transformations, the Hamiltonian becomes

$$F = H_e + F_{LO} + F_{IO}, \quad (22)$$

where

$$F_{LO} = \sum_k \frac{\hbar^2}{2m_e^*}k^2\eta_{LO}^2 + \frac{\hbar^2}{2m_e^*}\left(\sum_{k,m,p}|f_{m,p}(k)|^2 k\right)^2 + \sum_{k,m,p}|f_{m,p}(k)|^2\left[\hbar\omega_{LO} + \frac{\hbar^2k^2}{2m_e^*} - \frac{\hbar^2}{m_e^*}K_\rho k\right] + \frac{\hbar^2}{m_e^*}\left[\sum_{k,m,p}|f_{m,p}(k)|^2k^2\eta_{LO}\right] + \sum_k\left[\hbar\omega_{LO} - \frac{\hbar^2}{m_e^*}K_\rho k\right]\eta_{LO} + \sum_k\left[A^*\left[\sum_{m=1,3,..}^{\frac{N}{2}}\frac{\cos(\frac{m\pi z}{L})}{\left[k^2 + \left(\frac{m\pi}{L}\right)^2\right]^{\frac{1}{2}}}f_{m,+}(k) + \sum_{m=2,4,..}^{\frac{N}{2}}\frac{\sin\left(\frac{m\pi z}{L}\right)}{\left[k^2 + \left(\frac{m\pi}{L}\right)^2\right]^{\frac{1}{2}}}f_{m,-}(k)\right] + H.c.\right], \quad (23)$$

and

$$F_{IO} = \sum_{q,\sigma,p}\frac{\hbar^2}{2m_e^*}q^2\eta_{\sigma p}^2 + \frac{\hbar^2}{2m_e^*}\left(\sum_{\sigma,p,q}|g_{\sigma,p}(q)|^2 q\right)^2 + \sum_{q,\sigma,p}|g_{\sigma,p}(q)|^2\left[\hbar\omega_{\sigma p} + \frac{\hbar^2q^2}{2m_e^*} - \frac{\hbar^2}{m_e^*}K_\rho q\right] + \frac{\hbar^2}{m_e^*}\left[\sum_{q,\sigma,p}|g_{\sigma,p}(q)|^2q^2\eta_{\sigma p}\right] + \sum_q\left[\hbar\omega_{\sigma p} - \frac{\hbar^2}{m_e^*}K_\rho q\right]\eta_{\sigma p} + \sum_{q,\sigma}[W_{\sigma,+}(q,z)g_{\sigma,+}(q) + W_{\sigma,-}(q,z)g_{\sigma,-}(q) + H.c.] \quad (24)$$

$F_{LO}$ and $F_{IO}$ are, respectively, the contributions of the confined LO phonons and Interface phonons to the transformed Hamiltonian. $K_\rho$ is the component of the electronic wave vector in the $xy$-plane.

$$I_{\sigma+}=\int_0^{\frac{\pi}{2aU_{\sigma+}}}\frac{x\cosh^2(U_{\sigma+}xz)dx}{\omega_{\sigma+}^2\left(2\xi_{1\sigma+}^2\tanh\left(\frac{U_{\sigma+}xL}{2}\right)+2\xi_{2\sigma+}^2\right)(1+x^2+2x^2\eta_{\sigma+})^3\cosh^2\left(\frac{U_{\sigma+}xL}{2}\right)}, \tag{32}$$

$$I_{\sigma-}=\int_0^{\frac{\pi}{2aU_{\sigma-}}}\frac{x\sinh^2(U_{\sigma-}xz)dx}{\omega_{\sigma-}^2\left(2\xi_{1\sigma-}^2\coth\left(\frac{U_{\sigma-}xL}{2}\right)+2\xi_{2\sigma-}^2\right)(1+x^2+2x^2\eta_{\sigma-})^3\sinh^2\left(\frac{U_{\sigma-}xL}{2}\right)}; \tag{33}$$

According to the consideration of Lee-Low-Pines, and taking into consideration that only preferred direction in the $xy$-plane is the direction of $K_\rho$, we may introduce parameters $\lambda_1$ and $\lambda_2$

$$\sum_{k,m,p}|f_{m,p}(k)|^2k=\lambda_1K_\rho, \tag{25}$$

$$\sum_{q,\sigma,p}|g_{\sigma,p}(q)|^2q=\lambda_2K_\rho. \tag{26}$$

The variational conditions $(\partial F)/(\partial f_{m,p}(k))=0$, $(\partial F)/(\partial f_{m,p}^*(k))=0$, $(\partial F)/(\partial g_{\sigma,p}(q))=0$ and $(\partial F)/(\partial g_{\sigma,p}^*(q))=0$ are used to determine the expressions of $f_{m,p}(k)$, $f_{m,p}^*(k)$, $g_{\sigma,p}(q)$ and $g_{\sigma,p}(q)^*$.

It is necessary to point out that we are interested only in the analysis of slow electrons as observed in experiment, namely, we can set $K_\rho\approx 0$. By putting $f_{m,p}(k)$, $g_{\sigma,p}(q)$ and their conjugate formulas into equations (23, 24) and expanding them to the first power of $K_\rho$, $\lambda_1$ and $\lambda_2$ are found on the form:

$$\lambda_1=\frac{\alpha G(z)}{1+\alpha G(z)}, \tag{27}$$

$$G(z)=\frac{8}{Lk_{LO}}\left[\sum_{m=1,3..}^{\frac{N}{2}}\cos^2\left(\frac{m\pi z}{L}\right)I_m+\sum_{m=2,4..}^{\frac{N}{2}}\sin^2\left(\frac{m\pi z}{L}\right)I_m\right] \tag{28}$$

and

$$I_m=\int_0^\infty\frac{x^3dx}{(1+x^2+4x^2\eta_{LO})^3\left(x^2+\left(\frac{m\pi}{Lk_{LO}}\right)^2\right)}, \tag{29}$$

$$\lambda_2=\frac{\alpha V(z)}{1+\alpha V(z)}, \tag{30}$$

$$V(z)=\frac{4\omega_{LO}}{\pi\hbar k_{LO}}\left(\frac{1}{\epsilon_\infty}-\frac{1}{\epsilon_0}\right)^{-1}\sum_\sigma(I_{\sigma+}+I_{\sigma-}), \tag{31}$$

with

*see equation (32) above*

*see equation (33) above*

$\epsilon_0(\epsilon_\infty)$, $\alpha$ and $k_{LO}(U_{\sigma p})$ are, respectively, the static (optic) dielectric constant, the coupling constant of the electron-LO-phonon interaction, and the polaron wave vector for the LO-(IO-) phonons:

$$\alpha=\frac{m_e^*e^2}{\hbar^2k_{LO}}\left(\frac{1}{\epsilon_\infty}-\frac{1}{\epsilon_0}\right), \tag{34}$$

$$k_{LO}=\left(\frac{2m_e^*\hbar\omega_{LO}}{\hbar^2}\right)^{\frac{1}{2}}, \tag{35}$$

$$U_{\sigma p}=\left(\frac{2m_e^*\hbar\omega_{\sigma p}}{\hbar^2}\right)^{\frac{1}{2}}. \tag{36}$$

After minimizing $F$ with respect to $f_{m,p}(k)$ and $g_{\sigma,p}(q)$ we obtained the effective Hamiltonian $H_{eff}$ ($H_{eff}=\min F$).

$$H_{eff}=H_e^{'}+\frac{\hbar^2}{2m_e^*}K_\rho^2(1+\lambda_1^2+\lambda_2^2-2\lambda_1-2\lambda_2)+V_{e-LO}(z)+V_{e-IO}(z), \tag{37}$$

where $H_e^{'}=H_e-\hbar^2/(2m_e^*K_\rho^2)$. $V_{e-LO}(z)$ and $V_{e-IO}(z)$ are the effective potentials induced by the interaction between the electron and confined LO-phonons and IO-phonons, respectively:

$$V_{e-LO}(z)=\eta_{LO}\hbar\omega_{LO}-\frac{4\alpha\hbar\omega_{LO}}{Lk_{LO}}\times\left[\sum_{m=1,3,..}^{\frac{N}{2}}\frac{k_{LO}^2\cos^2\left(\frac{m\pi z}{L}\right)}{\left[(1+2\eta_{LO})\left(\frac{m\pi}{L}\right)^2-k_{LO}^2\right]}\log\left((1+2\eta_{LO})\left(\frac{m\pi}{Lk_{LO}}\right)^2\right)+\sum_{m=2,4,..}^{\frac{N}{2}}\frac{k_{LO}^2\sin^2(\frac{m\pi z}{L})}{\left[(1+2\eta_{LO})\left(\frac{m\pi}{L}\right)^2-k_{LO}^2\right]}\log\left((1+2\eta_{LO})\left(\frac{m\pi}{Lk_{LO}}\right)^2\right)\right], \tag{38}$$

$$V_{e-IO}(z)=\frac{-3\alpha}{\pi}\hbar\omega_{LO}\left(\frac{1}{\epsilon_\infty}-\frac{1}{\epsilon_0}\right)^{-1}\left[\sum_{\sigma+}\frac{I_1}{\hbar\omega_{\sigma+}^2}+\sum_{\sigma-}\frac{I_2}{\hbar\omega_{\sigma-}^2}\right]+\frac{S}{4\pi^2}\sum_{\sigma,p}U_{\sigma p}\int_0^{\frac{\pi}{2aU_{\sigma p}}}\eta_{\sigma p}\hbar\omega_{\sigma p}dx, \tag{39}$$

$$I_1 = \int_0^{\frac{\pi}{2aU_{\sigma+}}} \frac{\cosh^2(U_{\sigma+}xz)dx}{x\left(2\xi_{1\sigma+}^2 \tanh\left(\frac{U_{\sigma+}xL}{2}\right) + 2\xi_{2\sigma+}^2\right)(1+x^2+2x^2\eta_{\sigma+})\cosh^2\left(\frac{U_{\sigma+}xL}{2}\right)}, \quad (40)$$

$$I_2 = \int_0^{\frac{\pi}{2aU_{\sigma-}}} \frac{\sinh^2(U_{\sigma-}xz)dx}{x\left(2\xi_{1\sigma-}^2 \coth\left(\frac{U_{\sigma-}xL}{2}\right) + 2\xi_{2\sigma-}^2\right)(1+x^2+2x^2\eta_{\sigma-})\sinh^2\left(\frac{U_{\sigma-}xL}{2}\right)}. \quad (41)$$

*see equation (40) above*

*see equation (41) above*

In order to calculate the energies, the wave function of the electron is chosen in the form:

$$\phi_e(\vec{r}) = N_c f(z) g_{m,n}(\rho,\varphi); \quad (42)$$

$N_c$ is the normalization constant, $f(z)$ stands for the system wave function in the $nth$ well and the $nth$ barrier (solution of the periodic well) [27] and $g_{m,n}(\rho,\varphi)$ describes the electron motion in the $xy$-plane in the presence of the magnetic field:

$$g_{m,n}(\rho,\varphi) = \left[\frac{m_e^*\omega_c n!}{\hbar(n+m)!}\right]^{\frac{1}{2}} \exp(-im\varphi)\left[\frac{m_e^*\omega_c}{2\hbar}\right]^{\frac{m}{2}} \times \rho^m \exp\left(\frac{-m_e^*\omega_c\rho^2}{4\hbar}\right) L_{n+m}^m\left(\frac{m_e^*\omega_c\rho^2}{2\hbar}\right), \quad (43)$$

$n$ is the radial quantum number (Landau-level index) $n = 0, 1, 2, ...$ $m$ is the angular quantum number $m = 0, 1, 2, ...$ and $L_{n+m}^m(x)$ is the associated Laguerre polynomial of degree $(n+m)$ and order $m$

$$f(z) = \begin{cases} p^* \cosh\left[k_2\left(z - n(L+b) + \frac{L}{2}\right)\right] - q^* \sinh\left[k_2\left(z\right.\right. \\ \left.\left. -n(L+b) + \frac{L}{2}\right)\right] \\ \left(n - \frac{1}{2}\right)(L+b) < z < -\frac{L}{2} + n(L+b) \\ C' \exp(ik_1(z - n(L+b))) \\ +\beta \exp(-ik_1(z - n(L+b))) \\ -\frac{L}{2} + n(L+b) < z < \frac{L}{2} + n(L+b) \\ p\cosh\left[k_2\left(z - n(L+b) - \frac{L}{2}\right)\right] - q\sinh\left[k_2\left(z\right.\right. \\ \left.\left. -n(L+b) - \frac{L}{2}\right)\right] \\ \frac{L}{2} + n(L+b) < z < \frac{1}{2}(L+b), \end{cases} \quad (44)$$

$$k_1 = \left(\frac{m_w^*}{a_1'\hbar^2}\left[1 - (1 - 4a_1' E)^{\frac{1}{2}}\right]\right)^{\frac{1}{2}}, \quad (45)$$

$$k_2 = \left(\frac{m_b^*}{a_2'\hbar^2}[(1 + 4a_{13}(V_0 - E))^{\frac{1}{2}} - 1]\right)^{\frac{1}{2}}, \quad (46)$$

$$C' = K^+ \sinh(k_2 b); K^\pm = \frac{1}{2}\left[\frac{k_2}{k_1} \pm \frac{k_1}{k_2}\right], \quad (47)$$

$$\beta = \cosh(k_2 b)\sin(k_1 L) - K^- \sinh(k_2 b)\cos(k_1 L) + \sin[k_z(L+b)], \quad (48)$$

$$p = C' \exp\left(i\frac{k_1 L}{2}\right) + \beta \exp\left(-i\frac{k_1 L}{2}\right), \quad (49)$$

$$q = -i\frac{k_1}{k_2}\left(C' \exp\left(i\frac{k_1 L}{2}\right) - \beta \exp\left(-i\frac{k_1 L}{2}\right)\right), \quad (50)$$

with $a_{1(2)}' = [2m_{w(b)}^*/(\hbar^2)]^2 a_{13}$. The non-parabolicity affects the mass in the $xy$-plane, $m_{//}^* = m_w^* m_b^*/(P_w m_b^* + P_b m_w^*)$, 2–3 times more than that along the $z$-axis, not only because two degrees of freedom are concerned by Landau quantization, but also because of the band anisotropy [28]. $P_w(P_b)$ is the probability to find the electron inside (outside) the well. $m_w^*$ and $m_b^*$ are the electron effective mass in the well and in the barrier, respectively. The band gap energy $E_g$ is expressed as a function of the temperature [29]

$$E_g(T) = 2.887 - 0.07\left[1 + \frac{2}{\exp\left(\frac{248}{T}\right) - 1}\right]. \quad (51)$$

The magnetopolaron energy is determined as follows:

$$E_{mn} = \langle\phi_e(z,\rho)|H_{eff}|\phi_e(z,\rho)\rangle. \quad (52)$$

The cyclotron resonance mass can be obtained from the position of certain peaks in the magnetooptical absorption spectrum [5]. For that, we calculate the absorption coefficient and examine the variation of the peak position as a function of temperature in ZnCdSe/ZnSe MQWs. In the dipole approximation, the absorption coefficient $\alpha(\omega)$ for a linearly polarized electromagnetic wave in a medium of refractive index $n$ is given [30] by

$$\alpha(\omega) = \frac{4\pi}{ncm^*\omega V}\sum_{f,i}|\langle\psi_f|\vec{\varepsilon}\cdot\vec{P}|\psi_i\rangle|^2\delta(E_f - E_i - \hbar\omega), \quad (53)$$

$\vec{P}$ and $\hbar\omega$ are the electron momentum and the photon energy, respectively. The polarization vector $\vec{\varepsilon}$ defines the orientation of the electric field of the linearly polarized wave. The initial $|\psi_i\rangle$(occupied) and the final $|\psi_f\rangle$(empty) states of egenenergies $E_i$ and $E_f$ will be taken for the zero and the first Landau levels $E_{mn}$ (50), respectively.

The $\delta$-function is modelled by a narrow Lorentzian function

$$\delta(\omega) \to \frac{1}{\pi}\frac{\Gamma}{\omega^2 + \Gamma^2}. \quad (54)$$

We choose the width $\Gamma$ to be equal to 5 meV.

## 3 Results and discussion

The numerical calculations have been performed for ZnCdSe/ZnSe MQW with the following physical parameters [31]: $m_b^* = 0.155\, m_0$, $m_w^* = 0.140\, m_0$, $\epsilon_0 = 8.7$, $\epsilon_\infty = 5.73$ and $\hbar\omega_{LO} = 31.7$ meV.

The results presented in Figures 1 and 2 show the strong temperature dependence of the induced potentials

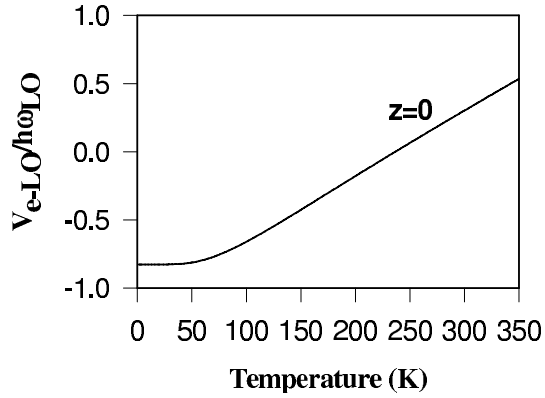


**Fig. 1.** The effective potential $V_{e-LO}(z=0)$ as a function of temperature for $L = 90$ Å and $b = 150$ Å.

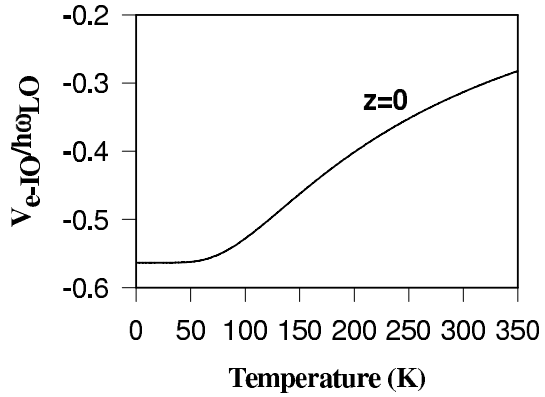


**Fig. 2.** The effective potential $V_{e-IO}(z=0)$ as a function of temperature for $L = 90$ Å and $b = 150$ Å.

$V_{e-LO}(z)$ (36) and $V_{e-IO}(z)$ (37). Both potentials increase with an increase of temperature, i.e., the self-trapping of the polaron will be enhanced with increasing temperature. We note that the augmentation of $V_{e-LO}(z)$ is more pronounced than that of $V_{e-IO}(z)$.

For the measurement scheme used in reference [9], where $\omega$ is fixed while the magnetic field varies, the cyclotron mass $m^*$ satisfies the relation

$$\frac{m^*}{m^*_{//}} = \frac{\overline{\omega}_c}{\omega} \tag{55}$$

where $\overline{\omega}_c$ is the cyclotron frequency, which corresponds to the cyclotron resonance peak in the magneto-optical absorption spectrum (Fig. 3). This figure shows the influence of the temperature on the optical absorption spectra. The optical absorption coefficient is displayed versus the cyclotron frequency $\omega_c$ for a fixed incident photon frequency ($\hbar\omega = 117$ meV) and different values of the temperature. The figure shows that the absorption peak is a non-monotonic function of the temperature. With increasing temperature, the peak first moves towards stronger magnetic fields, while at higher temperature there appears a shift towards weaker fields. This is still clearer in Figure 4, which displays the peak cyclotron frequency $\overline{\omega}_c$ as a function of the temperature. From this curve (Fig. 4), we can obtain $m^*(T)$ (Fig. 5) by means of the equation (53).

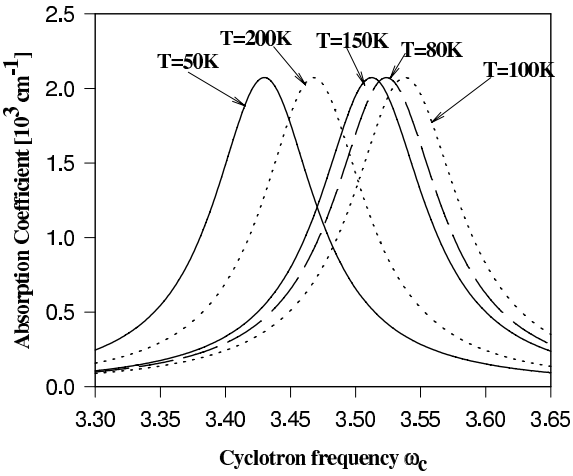


**Fig. 3.** Calculated magneto-absorption coefficient in ZnCdSe/ZnSe multi-QWs versus the cyclotron frequency, at the photon energy $\hbar\omega = 117$ meV, $L = 90$ Å, $b = 150$ Å and various temperatures.

From our calculations, we remark that there is an interplay between the electron-LO-phonon interaction, the electron-IO-phonon interaction and the band non-parabolicity of the conduction band. The effect of the different scattering mechanisms on the cyclotron mass can be, qualitatively, understood by analyzing the temperature dependence of the corresponding contributions to the transition energy $(E_1 - E_0)$. This is at a certain $\overline{\omega}_c$, which provides the maximum of the absorption coefficient, for a fixed photon frequency. From the equation (53) $m^*/m^*_{//} = \overline{\omega}_c/\omega = \hbar\overline{\omega}_c/\hbar\omega = (E_1 - E_0)/\hbar\omega$, we can see that an increase of $(E_1 - E_0)$ results in an increase of the cyclotron mass $m^*$. Figures 1 and 2 give a clear picture of the polaron effect contribution to the energy $(E_1 - E_0)$. We note that the induced potentials $V_{e-LO(IO)}(z)$ and $(E_1 - E_0)$ have qualitatively opposite behavior as a function of the temperature; namely: while $V_{e-LO(IO)}$ increases, the energy $(E_1 - E_0)$ decreases. We proved it numerically. At low temperatures $T < 95$ K, the optical phonons are less sensitive to the temperature fluctuation (see Figs. 1 and 2). This means that they do not affect strongly the dependence of the cyclotron mass on the temperature. In this case, the non-parabolicity of the conduction band is responsible for the increase of the cyclotron mass as a function of the temperature. Indeed, the band non-parabolicity influences the position of the energy levels and the electron has a lower transition energy than at high temperature (Eq. (51)). As pointed out by Huant et al. [28] for a cyclotron resonance measurement in quantum wells, the band non-parabolicity effects become important because of the electric confinement due to the band offset and magnetic field. Consequently, the cyclotron mass is affected by the non-parabolicity of the conduction band. At high temperatures $T > 95$ K electron-LO(-IO)-phonon interactions become dominant (see Figs. 1 and 2), that explains the decrease of the cyclotron resonance mass of magnetopolaron as the temperature rises. This result is consistent with that of Wei and

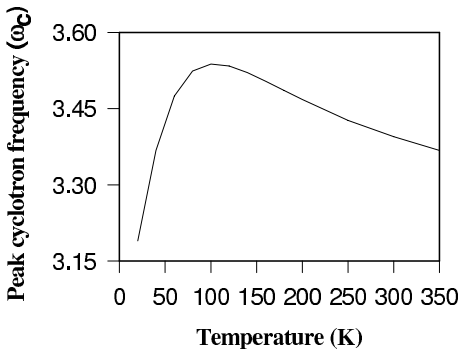


**Fig. 4.** Calculated peak cyclotron frequency $\varpi$ in ZnCdSe/ZnSe multi-QWs versus the temperature for $L$ = 90 Å and $b = 150$ Å.

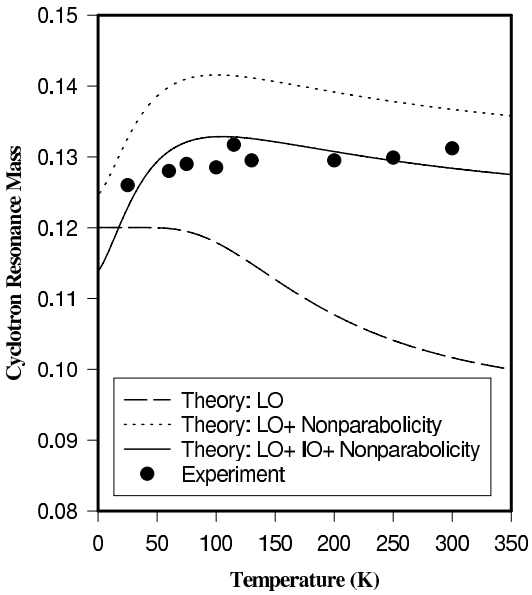


**Fig. 5.** Cyclotron mass, obtained from the calculated magneto-absorption spectra of polarons in ZnCdSe/ZnSe multi-QWs as a function of the temperature for $L = 90$ Å and $b = 150$ Å. The experimental data [9].

Kim [12] obtained using the Green's function method. We note that, in this range of the temperature, the polaron effect prevails over the non-parabolicity of the conduction band.

In Figure 5, the temperature dependence of the calculated cyclotron mass is plotted together with the experimental data (solid dots) of reference [9]. Taking into account only the electron-confined LO-phonon interaction, the cyclotron mass remains constant for $T < 95$ K but it decreases when $T > 95$ K. This result is consistent with other theoretical work [12] for high magnetic field. The nonparabolicity of the conduction band has an important impact especially at low temperatures. At high magnetic field, the electron-IO phonon interaction reduces the values of cyclotron mass. The interplay between the electron-LO(-IO)-phonon interaction and the non-parabolicity of the conduction band determines this behavior of the cyclotron mass as a function of temperature. By comparing with the experiment, we notice that the calculated cyclotron mass is in agreement with the experiment data for ZnCdSe/ZnSe MQWs.

We expect that the inclusion of the screening effect and the interaction of electrons with acoustic phonons, via the deformation potential, in our model will improve further the agreement between the calculation and the experimental results.

## 4 Conclusion

With the use of the L.L.P variational method, we have calculated the magnetopolaron cyclotron resonance mass in ZnCdSe/ZnSe MQWs at a high magnetic field with taking into account the nonparabolicity of the conduction band and the interaction of an electron with both confined LO- and IO-phonons. We show the theoretical temperature dependence of the cyclotron mass $m^*$, obtained from the position of the cyclotron resonance peak in the calculated absorption spectra at $\hbar\omega = 117$ meV. The curve $m^*$ versus $T$ displays a rather well pronounced maximum around $T \approx 95$ K. The calculated cyclotron mass $m^*(T)$ is in agreement with the experimental data [9]. This fact provides support for our interpretation of the observed non-monotonic temperature dependence of the cyclotron mass at a high magnetic field as being caused by the interplay between the electron-LO(-IO)-phonon interaction and the non-parabolicity of the conduction band.

## References

1. M.A. Haase, J. Qui, J.M. DePuydt, H. Cheng, Appl. Phys. Lett. **59**, 1272 (1991)
2. S. Wang, I. Huksson, J. Simpson, H. Stewart, S. Adams, J. Wallace, Y. Kawakami, K. Prior, B. Cavenett, Appl. Phys. Lett. **61**, 506 (1992)
3. M. Horinen, J. Ding, A. Nurmikko, D. Grillo, L.H.J. Han, R. Gunshor, Appl. Phys. Lett. **63**, 3128 (1993)
4. S. Taniguchi, T. Hino, S. Itoh, K. Nakayama, A. Ishibashi, M. Ikeda, Electron. Lett. **32**, 552 (1996)
5. F.M. Peeters, J.T. Devreese, Phys. Rev. B **34**, 7246 (1986)
6. Y. Imanaka, N. Muira, H. Nojiri, Physica B **246**, 328 (1998)
7. Y. Imanaka, N. Muira, H. Kukimoto, Phys. Rev. B **49**, 16965 (1994)
8. Y. Imanaka, N. Muira, Phys. Rev. B **50**, 14065 (1994)
9. Y. Imanaka, N. Muira, Physica B **249**, 932 (1998)
10. J.T. Devreese, V.M. Fomin, V. Gladilin, Y. Imanaka, N. Muira, J. Crys. Growth. **214/215**, 465 (2000)
11. J.T. Devreese, V.M. Fomin, V. Gladilin, Y. Imanaka, N. Muira, Physica B **298**, 207 (2001)
12. B.H. Wei, C.S. Kim, J. Phys.: Condens. Matter **10**, 4857 (1998)
13. B.H. Wei, S.W. Gu, Phys. Rev. B **43**, 9190 (1991)
14. Y. Osaka, J. Phys. Soc. Jpn **21**, 423 (1966)
15. G.Q. Hai, F.M. Peeters, J.T. Devreese, Phys. Rev. B **47**, 110358 (1993)

16. G.Q. Hai, F.M. Peeters, J.T. Devreese, Phys. Rev. B **48**, 4666 (1993)
17. D.L. Lin, R. Chen, T.F. George, Phys. Rev. **43**, 9328 (1991)
18. Y.J. Wang, H.A. Nickel, B.D. McCombe, F.M. Peeters, J.M. Shi, G.Q. Hai, X.G. Wu, T.J. Eustis, W. Schaff, Phys. Rev. Lett. **79**, 3226 (1997)
19. T.D. Lee, F. Low, D. Pines, Phys. Rev. **90**, 297 (1953)
20. M. Braun, U. Rossler, J. Phys. C: Solid State Phys. **18**, 3365 (1985)
21. P.Y. Yu, M. Cardona, *Fundamentals of Semiconductors: Physics and Materials Properties*, 3rd edn. (Springer, 1988)
22. L. Wendler, R. Pechstedt, Phys. Status Solidi B **141**, 129 (1987)
23. J.J. Licari, R. Evrard, Phys. Rev. B **15**, 2254 (1977)
24. R. Zheng, S. Ban, X.X. Liang, Phys. Rev. B **49**, 1796 (1994)
25. M.A. Brummell, R.J. Nicholas, M.A. Hopkins, J.J. Harris, C.T. Foxon, Phys. Rev. Lett. **58**, 77 (1987)
26. Y.C. Li, S.W. Gu, J. Phys: Condens. Matter **1**, 3201 (1989)
27. D. Elhabti, P. Vasilopoulos, J. Currie, Can. J. Phys. **68**, 268 (1990)
28. S. Huant, A. Mandray, B. Etienne, Phys. Rev. B **46**, 2613 (1992)
29. R. Granger, J.T. Benhlal, O. Ndap, R. Triboulet, Eur. Phys. J. B **13**, 429 (2000)
30. G. Bastard, *Wave Mechanics Applied to Semiconductor Hetero-structures* (Les Éditions de Physique, Les Ulis, 1988)
31. A.D. Nardis, V. Pellegrini, R. Colombelli, F. Beltram, L. Vanzetti, A. Franciosi, I. Krivorotov, K. Bajaj, Phys. Rev. B **61**, 1700 (2000)